INSTITUTE OF PHYSICS PUBLISHING PLASMA PHYSICS AND CONTROLLED FUSION

Plasma Phys. Control. Fusion **43** (2001) A237–A249 PII: S0741-3335(01)29546-3

Physics of the compact advanced stellarator NCSX

M C Zarnstorff[1], L A Berry[2], A Brooks[1], E Fredrickson[1], G-Y Fu[1], S Hirshman[2], S Hudson[1], L-P Ku[1], E Lazarus[2], D Mikkelsen[1], D Monticello[1], G H Neilson[1], N Pomphrey[1], A Reiman[1], D Spong[2], D Strickler[2], A Boozer[3], W A Cooper[4], R Goldston[1], R Hatcher[1], M Isaev[5], C Kessel[1], J Lewandowski[1], J F Lyon[2], P Merkel[6], H Mynick[1], B E Nelson[2], C Nuehrenberg[6], M Redi[1], W Reiersen[1], P Rutherford[1], R Sanchez[7], J Schmidt[1] and R B White[1]

[1] Princeton Plasma Physics Laboratory, Princeton, NJ 08543, USA
[2] Oak Ridge National Laboratory, Oak Ridge, TN 37831, USA
[3] Columbia University, New York, NY 10027, USA
[4] Ecole Polytechnique Federale de Lausanne, Lausanne, Switzerland
[5] Kurchatov Institute, Moscow, Russia
[6] Max Planck Institute for Plasma Physics, Greifswald, Germany
[7] Universidad Carlos III de Madrid, Spain

E-mail: zarnstorff@pppl.gov

Received 22 June 2001
Published 22 November 2001
Online at stacks.iop.org/PPCF/43/A237

Abstract

Compact optimized stellarators offer novel solutions for confining high-β plasmas and developing magnetic confinement fusion. The three-dimensional plasma shape can be designed to enhance the magnetohydrodynamic (MHD) stability without feedback or nearby conducting structures and provide drift-orbit confinement similar to tokamaks. These configurations offer the possibility of combining the steady-state low-recirculating power, external control, and disruption resilience of previous stellarators with the low aspect ratio, high β limit, and good confinement of advanced tokamaks. Quasi-axisymmetric equilibria have been developed for the proposed National Compact Stellarator Experiment (NCSX) with average aspect ratio 4–4.4 and average elongation $\sim$1.8. Even with bootstrap-current consistent profiles, they are passively stable to the ballooning, kink, vertical, Mercier, and neoclassical-tearing modes for $\beta > 4\%$, without the need for external feedback or conducting walls. The bootstrap current generates only 1/4 of the magnetic rotational transform at $\beta = 4\%$ (the rest is from the coils); thus the equilibrium is much less non-linear and is more controllable than similar advanced tokamaks. The enhanced stability is a result of 'reversed' global shear, the spatial distribution of local shear, and the large fraction of externally generated transform. Transport simulations show adequate fast-ion confinement and thermal neoclassical transport similar to equivalent tokamaks. Modular coils have been designed which reproduce the physics properties, provide good flux surfaces, and allow flexible variation of the plasma shape to control the predicted MHD stability and transport properties.

1. Introduction

Magnetic plasma confinement in toroidal geometries is well established and promising as a basis for future fusion reactors. Tokamaks, and other axisymmetric configurations, produce the confining poloidal magnetic field by toroidal currents in the plasma, which are typically generated inductively. Tokamaks have demonstrated excellent short-pulse plasma performance in 'compact' geometries, with aspect ratios (ratio of the plasma major radius to the average minor radius) usually less than 4. Stellarators use three-dimensional magnetic fields generated by coils to produce some or all of the confining poloidal magnetic field. Stellarators have demonstrated levels of performance approaching those of tokamaks, but generally at aspect ratios in the range of 6–12.

Since stellarators can produce all components of the magnetic field directly from external coils, they are intrinsically well suited for steady-state operation and do not require external current drive systems. In addition, stellarators typically do not experience disruptive terminations (disruptions) of the plasma. For example, both the W7-A [1] and Cleo [2] experiments were able to eliminate disruptions at the density limit and when passing through edge $q = 2$ (rotational transform $\iota = 0.5$) by the addition of small amounts of externally (coil) generated rotational transform to plasmas with substantial parallel plasma currents. Recent hybrid experiments on W7-AS [3,4] with induced toroidal current have generated disruptions at edge $\iota \sim 0.5$ ($q \sim 2$) when the plasma current profile is analysed to be unstable to global tearing modes (extending from centre to edge). This instability is well understood in both stellarators and tokamaks, and can be avoided either by design or care in experiment operation. Extending the study of stellarator stability and disruption avoidance to high β and low aspect ratio awaits new experiments.

As in tokamaks, the shape of the three-dimensional magnetohydrodynamic (MHD) equilibrium determines the physics properties of a stellarator. Three-dimensional equilibria offer many more degrees of freedom than are available for axisymmetric configurations and this additional shaping flexibility can be used to tailor the equilibrium to obtain desired physics properties. This was first systematically exploited in the development of the 'Advanced Stellarator' (AS) concept [5], in which a stellarator configuration was numerically optimized to realize good equilibrium, stability, and transport properties, using theoretical/numerical models. The AS optimization approach produced the designs for the Wendelstein 7-AS and Wendelstein 7-X [6] (under construction) experiments in Germany.

Historically, the major challenge for stellarators has been to provide acceptable drift-orbit confinement, allowing low neoclassical transport losses and adequate fast-ion confinement. This is due to the fully three-dimensional shape, which has no ignorable coordinates and thus no conserved canonical momenta for drift orbits. As a consequence, the radial excursion of drift orbits is not necessarily bounded as it is in axisymmetric systems. In addition, a general three-dimensional magnetic field will have a strong modulation in the magnitude of B, $|B|$, in every direction, producing strong plasma flow damping in all directions. Two strategies were identified [7] to provide adequate drift-orbit and neoclassical confinement, and have become practical through numerical optimization. The first strategy minimizes the poloidal variation of the magnetic field strength. This minimizes the Pfirsch–Schlüter and bootstrap currents [8], and reduces the radial component of the ∇B drift. This strategy was developed in the design of Wendelstein 7-X, with aspect ratio 10.6, where the orbit confinement was specifically optimized to minimize the bootstrap current. This strategy, partially optimized, also underlies the design of Wendelstein 7-AS. It is being further developed at low aspect ratio in the design of the QPS experiment [9].

The second strategy for three-dimensional drift-orbit confinement is called 'quasi-symmetry', which is based upon work by Boozer [10] showing that drift-orbit topology and neoclassical transport depend only on the variation of $|B|$ within a flux surface, not on the dependence of the vector components of B. This was used by Nührenberg and co-workers [11,12] and Garabedian [13] to develop stellarators that, while three-dimensional in Euclidean space, have a direction (either helical or toroidal) of approximate symmetry of $|B|$ in (Boozer) flux coordinates. Perfect quasi-helical or quasi-axisymmetry can only be achieved on one flux surface [14], but the deviation from symmetry grows slowly away from that surface. Quasi-symmetric configurations have drift orbits similar to equivalent symmetric configurations, and thus similar to neoclassical transport. Rotation in the quasi-symmetric direction is also undamped, as in a symmetric configuration. The first experimental test of quasi-symmetry is the Helically Symmetric eXperiment (HSX) now operating at the University of Wisconsin [15].

In parallel, there have been tremendous advances in the understanding of tokamak experiments and the ability to manipulate tokamak plasmas. There has been a general confirmation of ideal MHD equilibrium and stability theory and neoclassical transport theory. Methods for stabilizing and manipulating turbulent transport (particularly for ions) have been developed, allowing the elimination of anomalous ion thermal and particle transport, and reduction of anomalous electron thermal transport. There is a general understanding of the importance of flow-shear stabilization as a mechanism for stabilizing ion turbulence. In addition, there are theoretical predictions that undamped turbulence-generated flows (zonal flows) [16] are significant in saturating turbulent transport at the levels observed.

Quasi-axisymmetric stellarators offer novel solutions for confining high-β plasmas by combining the best features of tokamaks and stellarators. They offer the possibility of combining the steady-state low-recirculating power, external control, and disruption resilience of the stellarator with the low aspect ratio, high β limit, and good confinement of the advanced tokamak. Using the three-dimensional shaping flexibility available in a stellarator, configurations can be designed that are MHD stable without nearby conducting structure, require no current drive at high-β , and have good orbit confinement. Quasi-axisymmetry gives good orbit and neoclassical confinement, similar to equivalent tokamaks, and reduced damping of toroidal rotation. The reduced damping may allow manipulation of the radial electric field via driven rotation and the full development of zonal flows, similar to tokamaks. In addition, quasi-axisymmetric plasmas have significant bootstrap current, reducing the rotational transform required from the external coils. The rotational transform profile produced by the three-dimensional shaping and bootstrap current can be designed to monotonically increase towards the plasma edge, like the core region of a 'reversed shear' advanced tokamak. This is predicted to stabilize neoclassical tearing modes, reduce equilibrium islands, and stabilize trapped-particle-driven modes. Quasi-axisymmetry is well suited for the design of low aspect ratio configurations, since low aspect ratio forces the $n = 0$, $m \geqslant 1$ Fourier coefficients of the magnetic field strength to be large, where n and m are the toroidal and poloidal mode numbers, respectively. Low aspect ratio configurations are attractive in order to minimize the cost of near-term experiments and the capital cost of possible future power plants.

These configurations are being studied for the design of the National Compact Stellarator Experiment (NCSX). It is proposed to study the physics of the β limit in compact stellarators, the role of three-dimensional shaping and externally generated transform in disruptions, and the ability to operate reliably without disruptions at the β limit with low collisionality and bootstrap-current consistent profiles. It will also test quasi-axisymmetric reduction of neoclassical transport, the residual flow damping, effects on turbulence, and the ability to induce enhanced confinement. Compact quasi-axisymmetric stellarators are also being investigated for the design of the CHS-qa experiment [17].

2. Configuration design and stability

The basic procedure used is similar to that developed for Wendelstein 7-X. A target fixed-boundary plasma equilibrium is designed to have the desired physics properties. Coils are then designed to reproduce the target equilibrium and to generate good flux surfaces. The flexibility of the coils is tested by examining free-boundary equilibria with different profiles or different desired physics properties.

The target plasma configuration is designed by adjusting the three-dimensional plasma boundary shape to achieve the desired physics properties, such as transport and MHD stability, building upon previous experience and understanding the role of shaping for tokamaks and stellarators [18,19]. For these studies, the plasma configuration has been designed to be ideal MHD stable at $\beta = 4.25\%$, have a monotonically increasing ι profile (decreasing q profile), and be consistent with the bootstrap current while optimizing the quasi-axisymmetry of the magnetic field. An automated optimizer, used in these studies, calculates candidate three-dimensional equilibria using VMEC [20] and then directly evaluates kink stability (for $n \leqslant 7$ using TERPSICHORE [21]), ballooning stability (using COBRA [22] and TERPSICHORE), the bootstrap current, and plasma transport. Several methods have been implemented for evaluating the transport characteristics, including the magnitude of the non-symmetric Fourier components of the magnetic field strength, the effective magnetic ripple [23], Monte Carlo evaluation of fast-ion confinement, and a DKES [24, 25] calculation of mono-energetic particle transport. In addition, the optimizer can evaluate approximate coil characteristics (using NESCOIL [26]) to encourage realizable configurations.

A wide region of three-dimensional configuration space was explored, including aspect ratios from 3 to 5, edge rotational transform from 0.47 to 0.78, rotational transform fraction due to three-dimensional shaping from 50% to 80% , and from 2 to 4 periods. A broad pressure profile was assumed, within the range observed in existing stellarator experiments. The current profile was taken as the calculated bootstrap current, increased by 10% to provide margin against profile variation effects. A flat density profile was assumed for evaluating the bootstrap current. All of the configurations explored have large axisymmetric (or toroidal average) elongation and triangularity, to enable good stability to ballooning and kink modes. The vertical mode ($n = 0$) is calculated to be robustly stable [27], allowing consideration of average elongations up to 3. A large number of interesting configurations were found with good properties. These were then evaluated for flux surface quality, coil current density and complexity, and fast-ion confinement. To date, satisfactory coil designs have not been found for very large average elongations or very low aspect ratios.

Figure 1 shows the plasma boundary shape for the configuration adopted for the NCSX design. It has three field periods and an average aspect ratio $\langle A \rangle = R/\langle a \rangle = 4.4$, where R is the major radius and $\langle a \rangle$ is the average minor radius. This configuration is calculated to be passively stable to the ballooning, low-n external and internal kink, and vertical instabilities up to $\beta = 4.1\%$, without need for a conducting wall or active feedback systems. The rotational transform profile increases from 0.4 on axis to 0.66 near the plasma edge, dropping to 0.65 at the plasma edge. Approximately 1/4 of the edge rotational transform is from the bootstrap current and 3/4 is from the external coils. No external current drive is required. The bootstrap current is substantially smaller than in an equivalent advanced tokamak, due to the large transform from the coils. Due to the dominance of the coil-generated rotational transform, the equilibrium is less sensitive to the pressure profile shape than in an advanced tokamak. This should allow control of the equilibrium via the external coils.

The kink stability is calculated to be due to the high rotational transform, reduced bootstrap current density, and the spatial variation of the local magnetic shear [28]. A systematic

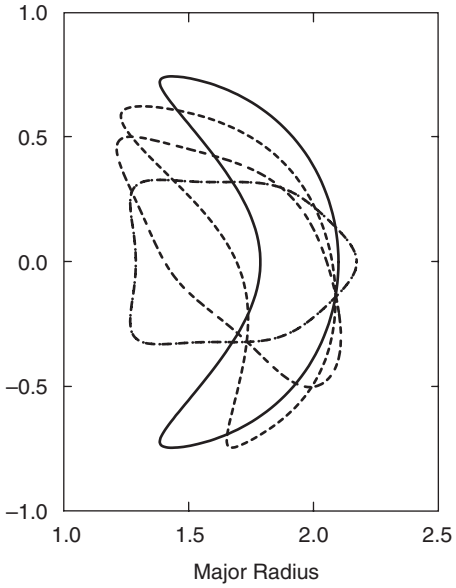

Figure 1. Plasma boundary shape in four poloidal cross-sections separated 20° toroidally.

convergence study of the stability of equilibrium shown in figure 1 using TERPSICHORE revealed a weak $n/m = 11/17$ instability localized to the plasma edge. Stability for all modes through $n \leqslant 20$ was achieved by a small modification of the plasma boundary shape. The passive vertical stability appears to be due to the substantial rotational transform produced by the external coils. Due to the rising rotational transform profile, neoclassical-tearing modes are theoretically stable over all but the plasma edge. Relative to earlier designs [29, 30] this configuration has higher rotational transform, higher average elongation and triangularity, simpler coils, and better quasi-axisymmetry (less helical ripple). The improved quasi-axisymmetry produced a marked improvement in the calculated neoclassical energy confinement and fast-ion orbit confinement.

The toroidally averaged shape is similar to an advanced tokamak, with an average elongation of 1.8 and an inside indentation of 9%. For this average shape, an equivalent current $I_{\mathrm{P}}^{\mathrm{Equiv}}$ can be defined as the current required to match the stellarator edge rotational transform in a tokamak with the same average shape. NCSX is envisioned to have $R = 1.42$ m, $\langle\, a \,\rangle = 0.33$ m, and B up to 1.7 T (at full external rotational transform). For these parameters, $I_{\mathrm{P}}^{\mathrm{Equiv}} = 0.71$ MA. Evaluating $\beta_{\mathrm{N}}^{\mathrm{Equiv}} = \beta/(I_{\mathrm{P}}^{\mathrm{Equiv}}/aB)$ gives $\beta_{\mathrm{N}}^{\mathrm{Equiv}} = 2.5$ for $\beta = 4.1\%$. Compared to advanced tokamaks, only moderate $\beta_{\mathrm{N}}^{\mathrm{Equiv}}$ is required due to the large $I_{\mathrm{P}}^{\mathrm{Equiv}}$ from the coil-generated rotational transform.

The quality of the flux surfaces for this configuration has been evaluated using the PIES equilibrium code [31]. Figure 2(*a*) shows the calculated fixed-boundary equilibrium flux surfaces for the equilibrium of figure 1, showing a significant $n/m = 3/5$ island, with a width of ∼10% of the minor radius and a smaller $n/m = 3/6$ island in the core. These calculations do not include neoclassical-healing effects, from suppression of the bootstrap current in the island. An analytic estimate of the neoclassical healing gives an expected island width of <5% of the plasma minor radius.

These islands have been removed from the equilibrium by modification of the plasma boundary shape [32]. A series of (short) PIES calculations is used to measure the change in island

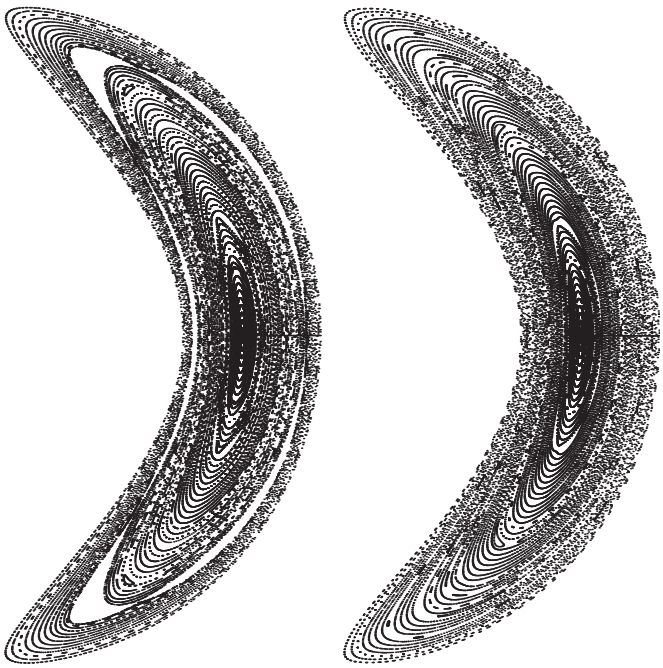

Figure 2. Poincaré plot of flux-surface structure: (*a*) original target plasma of figure 1, (*b*) with boundary perturbed to remove islands (fewer flux surfaces plotted).

widths due to perturbations of resonant Fourier components of the plasma boundary shape. The calculation of the resonant fields and island widths is via construction of quadratic-flux minimizing surfaces [33]. The coupling matrix is inverted to give the change in boundary shape required to remove the observed equilibrium islands. Using this algorithm, the $n/m = 3/4$, 3/5, 3/6, and 3/7 Fourier components of the boundary minor radius were perturbed by 4.2, 1.4, 3.2, and -1.1 mm, respectively. The resulting equilibrium, see figure 2(*b*), confirms that the 3/5 island was removed, though a small residual 6/10 island remains that was not targeted. The plasma stability and transport characteristics of the perturbed equilibrium have been analysed and found to be unchanged from the original design.

3. Confinement

The degree of quasi-axisymmetry can be characterized by the effective ripple strength $\varepsilon_{\mathrm{h,eff}}$ [23], calculated numerically to match the $1/\nu$ transport regime. As shown in figure 3, the effective ripple rises exponentially to $\sim$1.2% at the plasma edge. The toroidal spectrum of the ripple is dominated by low-order perturbations, $n = 3$ and 6 as shown in figure 4, which reduces its effect on confinement relative to typical tokamak ripple with $n \sim 20$. This low $\varepsilon_{\mathrm{h,eff}}$, together with the relatively high rotational transform, results in acceptably low fast-ion losses, as calculated by Monte Carlo simulations [34] using the full three-dimensional magnetic field. The calculated energy losses of 40 keV H-neutral beam ions with $B = 1.7$ T are $\sim$15% for co-tangential injection and 23% for counter-injection. These counter-injection losses are similar to those for a tokamak of similar size and are low enough that balanced neutral beam

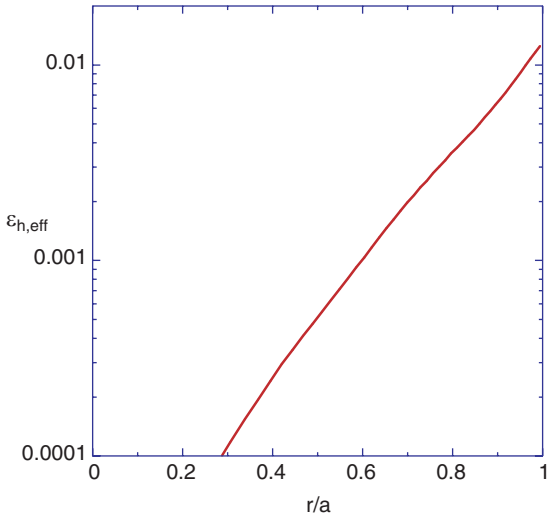

Figure 3. Radial profile of effective helical ripple.

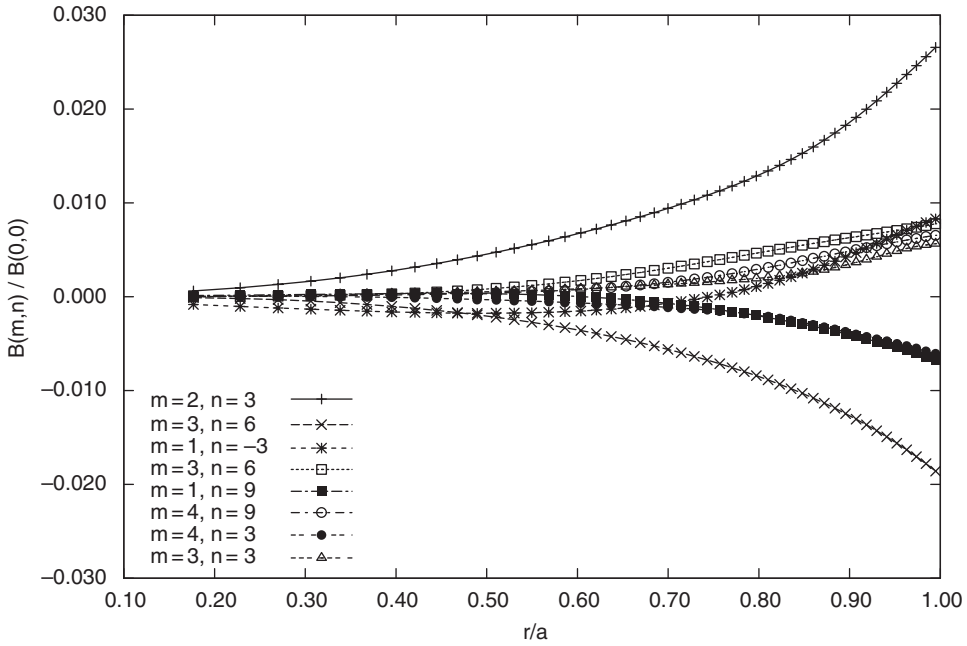

Figure 4. Radial profile of non-axisymmetric components of the magnetic field strength $|B|$ in Boozer coordinates.

injection can be envisioned to control the beam-driven current and to allow control of rotation. The calculated α-particle losses in a projected reactor are <20%, including collisional effects, depending on the final size.

The thermal transport is assessed in two ways. The neoclassical confinement is calculated for specified profiles by Monte Carlo simulation using the GTC code [35]. The code simulates the full ion distribution function (f) and the deviation of the electron distribution from a

Maxwellian (δf). It calculates the ambipolar electric field via a low-noise technique [36] for calculating the particle fluxes from the toroidal variation of $p_\parallel + p_\perp$. The second method combines models of the transport processes (helical neoclassical, toroidal neoclassical, anomalous) in a one-dimensional transport solver (STP) to predict temperature profiles and confinement for an assumed density profile. It includes an axisymmetric beam-deposition model and the Monte Carlo code calculated fast-ion losses. The model for helical ripple-neoclassical transport uses the calculated $\varepsilon_{\mathrm{h,eff}}$ and the Shaing–Houlberg full transport matrix [37]. Toroidal neoclassical transport is calculated following Chang–Hinton [38] normalized to a THRIFT/NCLASS [39] calculation averaging over the full three-dimensional equilibrium. Anomalous transport is simulated using either a spatially uniform diffusivity or the Lackner–Gottardi model [40]. STP calculates the ambipolar electric field, choosing the ion root if it exists. The code can vary the magnitude of the anomalous transport model to match the total confinement time to a global confinement scaling, such as ISS-95 [41] or ITER-97P [42], times an enhancement factor. For a specified heating power, it will vary the density and confinement enhancement factor to achieve a specified β value and collisionality, subject to an empirical density limit [43]. The two methods have been benchmarked and predict the same ambipolar electric field to within 5% and the same ion energy flux within the Monte Carlo simulation uncertainty.

The predicted plasma transport is dominated by the anomalous transport and the toroidal neoclassical losses. The predicted ripple thermal transport is negligible in all cases studied. As an example, figure 5 shows the predicted radial power flow and temperature profiles for a $\beta = 4\%$ plasma with a collisionality $\nu^* = 0.25$ at the half radius, using $B = 1.2\,\mathrm{T}$, 6 MW of neutral beam injected power, an average density of $6 \times 10^{19}\,\mathrm{m}^{-3}$, and spatially uniform anomalous transport coefficients. Note that the ripple-neoclassical flux is insignificant and that the anomalous transport dominates over most of the profile. Simulations using the Lackner–Gottardi model give similar results. The calculations indicate that achieving $\beta = 4\%$ with these parameters requires a global confinement time 2.9 times the ISS-95 scaling, somewhat higher than the best achieved on LHD and W7-AS. Since this configuration is designed to have tokamak-like drift orbits and the simulations predict tokamak-like transport, it is reasonable to compare this confinement to tokamak global scalings. If we use $I_{\mathrm{P}}^{\mathrm{Equiv}}$ to evaluate the

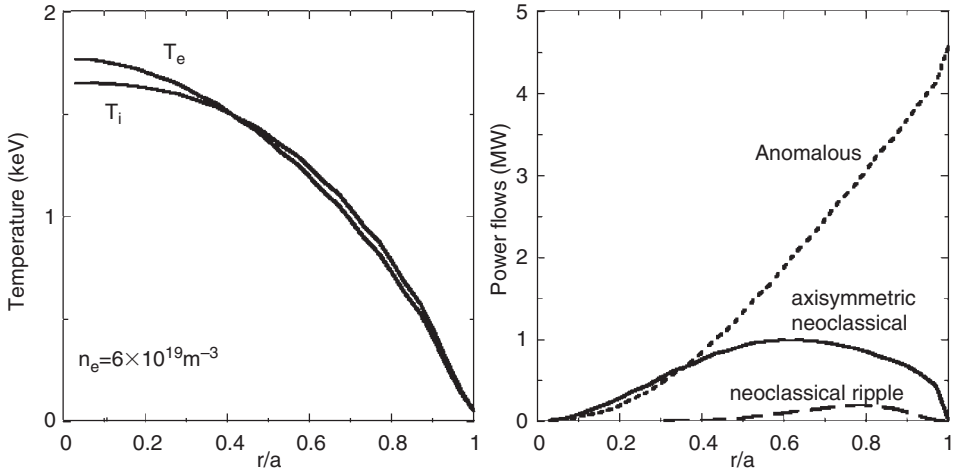

Figure 5. (*a*) Predicted T_{e} and T_{i} profiles, and (*b*) radial power flows for $B = 1.2\,\mathrm{T}$, $P = 6\,\mathrm{MW}$.

tokamak scaling, the required confinement to achieve $\beta = 4\%$ and $\nu^* = 0.25$ is $\sim$0.9 times the ITER-97P prediction. For comparison, similar-sized PBX-M plasmas achieved $\beta = 6.8\%$ with 5.5 MW of heating and $B = 1.1$ T achieving a confinement of 1.7 times the ITER-97P prediction or $\sim$3.9 times the ISS-95 prediction. Since ISS-95 and ITER-89P have different parametric dependencies, the confinement multipliers must be expected to vary separately. For the same conditions, except $B = 1.7$ T, STP predicts central temperatures of 2.3 keV, $\nu^* = 0.1$.

There are a number of reasons to expect that the confinement may be enhanced in this configuration, relative to standard stellarators and tokamaks. The high degree of quasi-symmetry should reduce flow damping, allowing development of persistent zonal flows. This may stabilize turbulence at lower levels than in non-symmetric stellarators. In addition, the 'reversed' shear should stabilize trapped-particle modes and eliminate the trapped-electron drive for ITG turbulence [44,45], similar to reversed-shear advanced tokamak regimes.

4. Coil design and flexibility

A wide range of coil topologies and designs have been explored for generating the equilibrium in figure 1, including modular, helical, and saddle coils, using a number of optimization strategies [46]. Of these, the modular coils (shown in figure 6) best reproduce the physics properties and good flux surfaces of the target equilibrium. These coils would be used with a set of poloidal field coils, to control plasma position and average shape, and a weak toroidal solenoid to allow variation of rotational transform. The modular coil design shown has seven coils per period, with four different coil shapes. The coils at the elongated symmetry plane have been extended radially to allow tangential neutral beam injection and to provide tangential diagnostic views. The coils do not reproduce the original fixed-boundary plasma shape precisely, but approximate it subject to engineering constraints on coil characteristics,

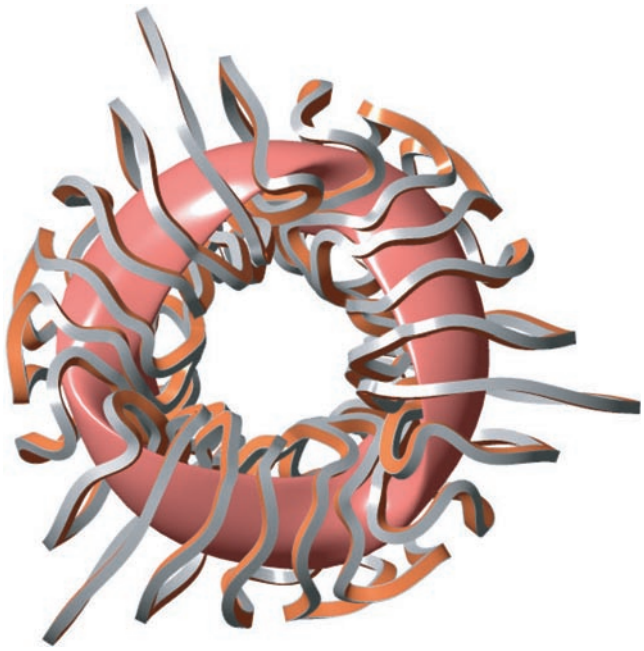

Figure 6. Optimized modular coils for the equilibrium of figure 1.

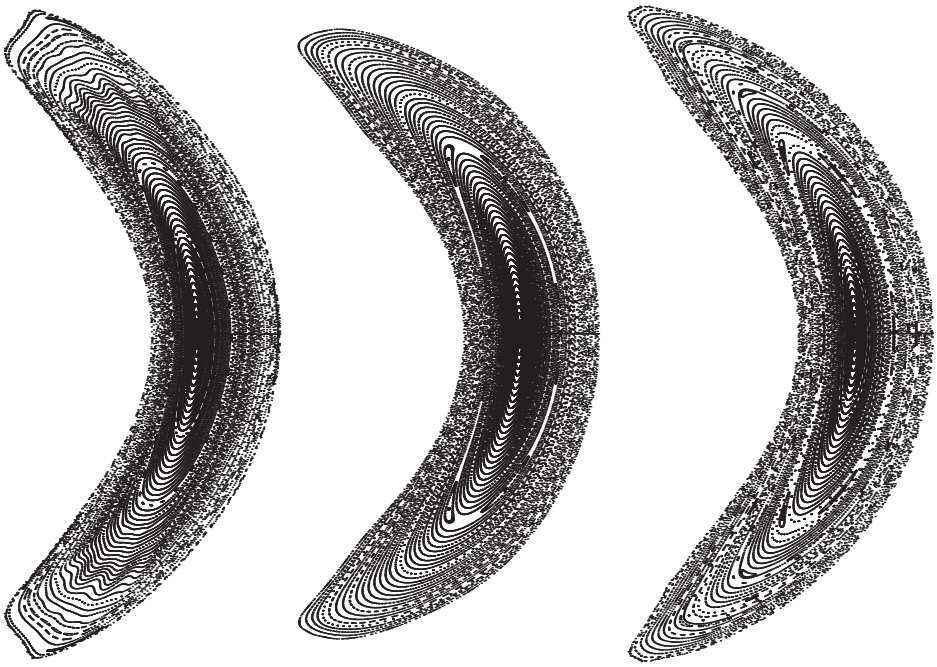

Figure 7. Poincaré plots of flux-surface structure for free-boundary equilibria: (*a*) vacuum, (*b*) $\beta = 2\%$, $I_P = 83\,\mathrm{kA}$, (*c*)$\beta = 4.1\%$ $I_P = 125\,\mathrm{kA}$. Current values correspond to $B = 1.2\,\mathrm{T}$.

such as bend radii and coil-separation distances. To test the adequacy of a coil design, the coil currents are re-optimized to achieve the original plasma criteria (MHD stability and quasi-axisymmetry) based on free-boundary equilibrium calculations. Free-boundary optimized equilibria have been found that reproduce the key properties of original fixed-boundary design.

The coils must not introduce large islands or stochastic field regions. The coil shapes are perturbed to remove resonant fields that produce islands, as calculated in a free-boundary PIES equilibrium. The algorithm is similar to that used for removing the fixed-boundary equilibrium islands, above. The resulting coils are calculated to be able to produce equilibria with good flux surfaces over a wide range of conditions, as shown in figure 7.

For an experiment, the coil system must robustly handle a variety of pressure and current profiles and be flexible to handle the discharge evolution and generate a variety of configurations for physics studies. This has been studied using the free-boundary optimizer to test whether a coil design can produce equilibria with specified properties. For these studies, it is assumed that the current in each coil type can be independently controlled (preserving stellarator symmetry). Figure 8 shows a study of the accessible range of edge rotational transform with the modular coils, for fixed pressure and plasma current, while optimizing quasi-axisymmetry and constraining the plasma to be within a design vacuum vessel. For the cases shown, the ripple magnitude is no more than 1.8 times the original optimized configuration. A wide range of operation is available, including configurations where the transform profile is entirely above or below 1/2. This flexibility will allow control of the edge rotational transform, if needed, preventing it from passing through 1/2 during the discharge evolution, thus avoiding the tearing modes and disruptions observed in hybrid operation of W7-AS [3, 4]. A similar study varied

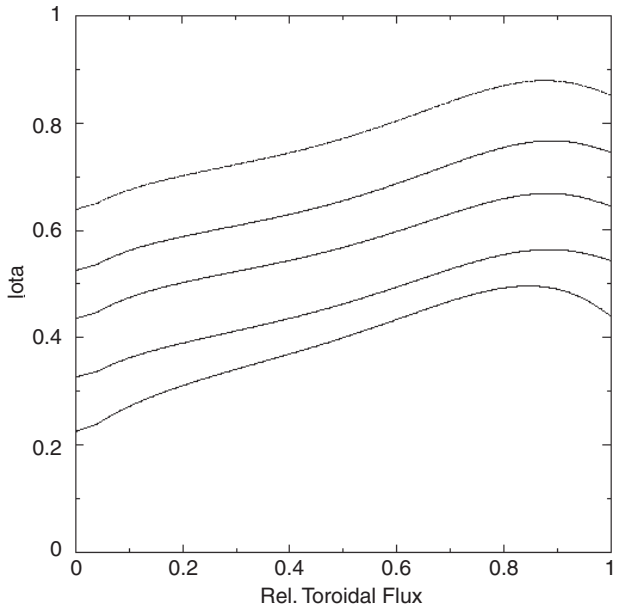

Figure 8. Free-boundary optimized variations of the rotational transform profile using modular coils, maintaining approximate quasi-symmetry, with fixed plasma pressure and current profiles.

the magnetic shear down to approximately shearless at full plasma current by varying the modular coil currents. In these cases, the quasi-symmetry was degraded by up to a factor of 5 (for the shearless case). A set of trim coils is planned to control low-order resonant field components and the islands they generate, to allow operation over a large range of magnetic transform profiles.

Accessible free-boundary equilibria have been found with substantially improved or degraded quasi-axisymmetry, for fixed plasma profiles and ι profile. Similarly, the kink β limit can be varied by at least a factor of 3 just by varying the plasma shape via external coil currents, either at fixed edge ι or with a fixed shear profile. This ability to manipulate the plasma characteristics will enable controlled experiments for comparison with theoretical predictions and testing models. Surprisingly, the β limit for free-boundary equilibria has not been found yet. Stable equilibria with $\beta > 6.5\%$ have been found with some degradation of the quasi-symmetry, but without yet making use of profile optimization.

The evolution of the plasma current from vacuum through an Ohmic current-ramp to equilibration with the bootstrap current has been simulated using an assumed temperature evolution. By assuming early auxiliary heating to increase the temperature, as used in reversed-shear tokamak experiments, broad current profiles were predicted which equilibrate with the bootstrap current in $\sim$0.4 s. The current evolution was approximated using an axisymmetric calculation, representing the rotational transform from the coils as a constant imposed external current drive profile. The calculated current profiles and pressure profiles were used with the free-boundary optimizer to calculate the evolution of coil currents constraining the plasma shape to stay approximately fixed. Simulation of the evolution from vacuum to $\beta = 4.25\%$ showed reasonable coil-current variations and that kink modes were calculated to be stable throughout the evolution. Stable evolution scenarios have been found where $\iota(a)$ either crosses 1/2 or is always above 1/2. In all cases studied, Δ' analysis indicates that the current profiles

are stable or marginally stable to tearing instabilities.

In simulations of unidirectional tangential neutral beam injection, the beam-driven current strongly changed the core rotational transform. For co-tangential-only injection, the central rotational transform rapidly goes above one, producing a tokamak-like shear profile, which is unstable to neoclassical-tearing modes. From these simulations, balanced co- and counter-injection will be required to obtain the optimized current profile. Variations away from balanced injection could be used to control the central magnetic shear.

5. Conclusions

A novel compact quasi-axisymmetric stellarator has been designed for NCSX, combining features from optimized stellarators and advanced tokamaks, and offering a possible path to steady-state reactors without current drive or disruptions. Extra design flexibility from three-dimensional shaping has been used to passively stabilize the kink, vertical, ballooning, Mercier, and neoclassical-tearing modes at $\beta > 4\%$ without need for external conducting walls or feedback, while maintaining good orbit confinement. The calculated confinement characteristics are similar to an equivalent tokamak. This NCSX design demonstrates the power of the recent advances in experimental and theoretical understanding and numerical modelling, and illustrates the possibilities available for magnetic confinement with three-dimensional shaping.

Acknowledgments

We gratefully acknowledge useful discussions with P Garabedian, C Hegna, H Maassberg and J Nührenberg. This research was supported by the US Department of Energy under contracts DE-AC-76-CH0-3073 and DE-AC05-00OR22725, by Euratom, and by the Fonds National Suisse de la Recherche Scientifique.

References

[1] W VII-A Team 1980 *Nucl. Fusion* **20** 1093
[2] Robinson D C and Todd T N 1982 *Phys. Rev. Lett.* **48** 1359
[3] Weller A *et al* 2001 *Fusion energy (Proc. 18th Int. Conf., Sorrento 2000)* EX714 (Vienna: IAEA)
[4] Sallander E, Weller A and W7-AS Team 2000 *Nucl. Fusion* **40** 1499
[5] Nührenberg J and Zille R 1986 *Phys. Lett.* A **114** 129
[6] Beidler C *et al* 1990 *Fusion Technol.* **17** 148
[7] Kovrizhnykh L M 1985 *Nucl. Fusion* **25** 1391
[8] Wobig H 1999 *Plasma Phys. Control. Fusion* **41** A159
[9] Spong D *et al* 2001 *Nucl. Fusion* **41** 711
[10] Boozer A 1983 *Phys. Fluids* **26** 496
[11] Nührenberg J and Zille R 1988 *Phys. Lett.* A **129** 113.
[12] Nührenberg J, Lotz W and Gori S 1994 *Theory of Fusion Plasmas* ed E Sidoni *et al* (Bologna: SIF)
[13] Garabedian P 1996 *Phys. Plasmas* **3** 2483
[14] Garren D A and Boozer A H 1991 *Phys. Fluids* B **3** 2805
[15] Anderson D T and Garabedian P R 1994 *Nucl. Fusion* **34** 881
[16] Rosenbluth M N and Hinton F L 1998 *Phys. Rev. Lett.* **80** 724
[17] Okamura S *et al* 2001 *Fusion Energy* (*Proc. 18th Int. Conf., Sorrento 2000*) ICP/16 (Vienna: IAEA)
[18] Reiman A *et al* 2001 *Phys. Plasmas* **8** 2083
[19] Garabedian P and Ku L-P 1999 *Phys. Plasmas* **6** 645
[20] Hirshman S P and Whitson J C 1983 *Phys. Fluids* **26** 3533
[21] Anderson D V *et al* 1990 *Int. J. Supercomput. Appl.* **4** 34
[22] Sanchez R *et al* 2000 *J. Comp. Phys.* **161** 589

[23] Nemov V V *et al* 1999 *Phys. Plasmas* **6** 4622
[24] Hirshman S P *et al* 1986 *Phys. Fluids* **29** 2951
[25] van Rij W I and Hirshman S P 1989 *Phys. Fluids* B **1** 563
[26] Merkel P 1987 *Nucl. Fusion* **27** 867
[27] Fu G Y *et al* 2000 *Phys. Plasmas* **7** 1809
[28] Fu G Y *et al* 2001 *Fusion Energy* (*Proc. 18th Int. Conf. Fusion Energy, Sorrento 2000*) TH3/2 (Vienna: IAEA)
[29] Reiman A *et al* 1999 *Plasma Phys. Control. Fusion* **41** B273
[30] Neilson G H *et al* 2000 *Phys. Plasmas* **7** 1911
[31] Reiman A H and Greenside H S 1988 *J. Comput. Phys.* **75** 423
[32] Hudson S R, Monticello D A and Reiman A H 2001 *Phys. Plasmas* **8** 3377
[33] Hudson S R and Dewar R L 1999 *Phys. Plasmas* **6** 1532
[34] Spong D A *et al Fusion Energy* (*Proc. 17th Int. Conf., Yokohama, 1998*) vol 3 (Vienna: IAEA) 1159
[35] Lin Z *et al* 1995 *Phys. Plasmas* **2** 2975
[36] Lewandowski J *et al* 2001 *Phys. Plasmas* **8** 2849
[37] Hastings D E *et al* 1985 *Nucl. Fusion* **25** 445
[38] Chang C S and Hinton F L 1986 *Phys. Fluids* **29** 3314
[39] Strand P I and Houlberg W A 2001 *Phys. Plasmas* **8** 2782
[40] Lackner K and Gottardi N A O 1990 *Nucl. Fusion* **30** 767
[41] Stroth U *et al* 1996 *Nucl. Fusion* **36** 1063
[42] Kaye S *et al* 1997 *Nucl. Fusion* **37** 1303
[43] Sudo S *et al* 1990 *Nucl. Fusion* **30** 11
[44] Kessel C *et al* 1994 *Phys. Rev. Lett.* **72** 1212
[45] Yokoyama M *et al* 2001 *Phys. Rev.* E **64** 15401
[46] Pomphrey N *et al* 2001 *Nucl. Fusion* **41** 339